Journal of Medicinal Chemistry

Article

pubs.acs.org/jmc

Structure–Activity Relationship Studies of Argiotoxins: Selective and Potent Inhibitors of Ionotropic Glutamate Receptors

Mette H. Poulsen,[†] Simon Lucas,[†,‡] Tinna B. Bach, Anne F. Barslund, Claudius Wenzler, Christel B. Jensen, Anders S. Kristensen, and Kristian Strømgaard*

Department of Drug Design and Pharmacology, University of Copenhagen, Universitetsparken 2, DK-2100 Copenhagen, Denmark

Supporting Information

ABSTRACT: Argiotoxin-636 (ArgTX-636), a natural product from the spider *Argiope lobata*, is a potent but nonselective open-channel blocker of ionotropic glutamate (iGlu) receptors. Here, three series of analogues were designed to exploit selectivity among iGlu receptors, taking advantage of a recently developed solid-phase synthetic methodology for the synthesis of ArgTX-636 and analogues. Initially, the importance of secondary amino groups in the polyamine chain was studied by the synthesis of systematically modified ArgTX-636 analogues, which were evaluated for pharmacological activity at NMDA and AMPA receptors. This led to the identification of two compounds with preference for NMDA and AMPA receptors, respectively. These were further elaborated by systematically changing the aromatic headgroup and linker amino acid leading to compounds with increased potency and selectivity for NMDA and AMPA receptors, respectively. Thus, the first structure–activity relationship study of ArgTX-636 has been carried out and has provided lead compounds for probing the ion channel region of iGlu receptors.

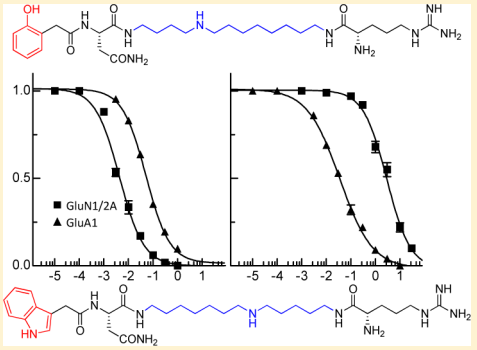

INTRODUCTION

The family of ionotropic glutamate (iGlu) receptors are ligand-gated ion channels that mediate the majority of excitatory synaptic transmission in the vertebrate brain and are crucial for normal brain function.[1−3] Dysfunction of iGlu receptors is involved in a range of neurological and psychiatric diseases, and iGlu receptors are considered important drug targets for brain diseases. In particular, inhibition of iGlu receptors is a promising strategy for the treatment of neurodegenerative diseases such as stroke and Alzheimer's disease.[1] However, development of selective and clinically effective iGlu receptor inhibitors has proven to be difficult, and today only a few drugs directed against iGlu receptors have been approved, one of which is memantine, an open-channel blocker of the *N*-methyl-D-aspartate (NMDA) subtype of iGlu receptors used in the treatment of Alzheimer's disease.[4−7]

Polyamine toxins are a group of small molecules found in spiders and wasps that like memantine are open-channel blockers of iGlu receptors.[8] Polyamine toxins have found valuable use as pharmacological tools based on their high affinity and selectivity for iGlu receptors,[8,9] particularly as they are uniquely selective for iGlu receptors, which are permeable to Ca^{2+}.[10,11] However, polyamine toxins have not yet been explored as templates for the development of iGlu receptor drugs, although the selective antagonism of Ca^{2+}-permeable iGlu receptors has been suggested as a particularly promising strategy in neuroprotection.[12−14] A main concern is that native polyamine toxins generally distinguish poorly among individual subtypes of iGlu receptors, such as NMDA and α-amino-3-hydroxy-5-methyl-4-isoxazolepropionic acid (AMPA) receptors.

Philanthotoxin-433 (PhTX-433, **1**, Figure 1) is the prototypical polyamine toxin[15] that has been studied in several structure–activity relationship (SAR) studies, where particularly the ease of synthesis by solid-phase synthetic (SPS) methodologies has been exploited and provided a large number of PhTX-433 derivatives, some of which particularly show increased selectivity for AMPA receptors.[16−23] Much less

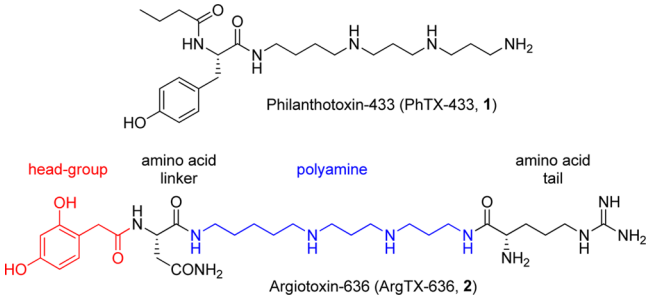

Figure 1. Structures of two prototypical polyamine toxins: philantoxin-433 (PhTX-433) isolated from the digger wasp *Philanthus triangulum* and argiotoxin-636 (ArgTX-636) isolated from the orb weaver spider *Argiope lobata*. ArgTX-636 can be divided into four structural regions, headgroup, linker amino acid, polyamine, and amino acid tail, which also relates to the biosynthetic origin.

Received: October 30, 2012
Published: January 2, 2013

dx.doi.org/10.1021/jm301602d | *J. Med. Chem.* 2013, 56, 1171−1181

Scheme 1. Synthesis of Compounds 3−9[a]

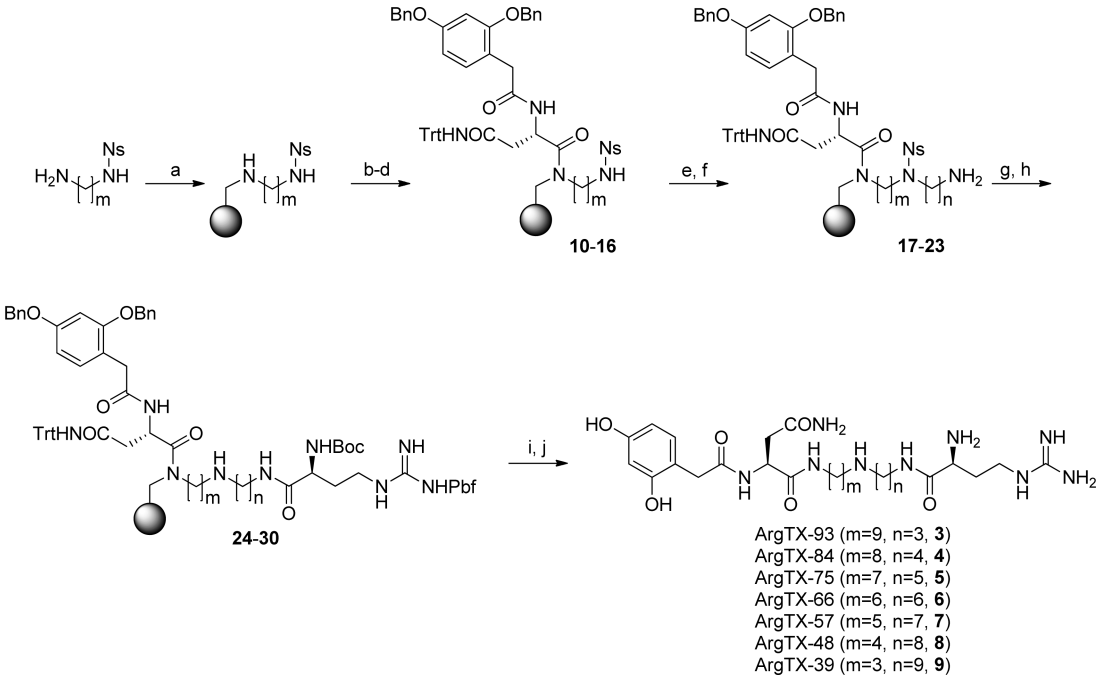

[a]Reagents and conditions: (a) 2-(3,5-dimethoxy-4-formylphenoxy)ethylpolystyrene, $NaBH(OAc)_3$, DMF/AcOH (9:1); (b) Fmoc-L-Asn(Trt)-OH, HATU, DIPEA; (c) 20% piperidine in DMF; (d) 2-(2,4-bis(benzyloxy)phenyl)acetic acid, HATU, DIPEA; (e) *N*-Teoc amino alcohol, Bu_3P, ADDP; (f) TBAF, 55 °C; (g) Fmoc-L-Arg(Pbf)-OH, HATU, DIPEA; (h) DBU, 2-mercaptoethanol; (i) TFA/DCM/TIPS/H_2O (75:20:2.5:2.5); (j) H_2, $Pd(OH)_2/C$.

attention has been focused on the wealth of spider polyamine toxins such as argiotoxin-636 (ArgTX-636, **2**, Figure 1) probably because of their increased structural complexity and hence more challenging synthetic feasibility.[24−26] However, several spider polyamine toxins are significantly more potent as iGlu receptor antagonists than PhTX-433, and some even display a certain degree of selectivity among iGlu receptor subtypes.[24] Thus, spider polyamine toxins are potentially superior starting points for development of pharmacological tools such as potent and subtype specific ligands for studies of iGlu receptors. ArgTX-636 (**2**) is a polyamine toxin isolated from the venom of the orb weaver spider *Argiope lobata*[24,25] and is one of the most potent inhibitors of iGlu receptors, which are blocked in a use- and voltage-dependent manner presumably by binding to the ion channel region of the receptors.[24] Toxin **2** has, similar to other channel blockers of iGlu receptors, demonstrated neuroprotective properties[27,28] and thus has the potential to be used as a template for developing therapeutically relevant compounds. However, the main challenge is that native **2** does not distinguish between subtypes of iGlu receptors.[1,8,9]

We have recently developed an efficient SPS methodology for the generation of **2** and derivatives, and in the same study we found a notable relationship between modification of the polyamine moiety of **2** and antagonistic selectivity among NMDA and AMPA receptors.[29] Initially, we found that modification of the guanidyl moiety was not tolerated, but changing either one of the secondary amino groups in the polyamine moiety led to increased selectivity for NMDA and AMPA receptors, respectively.[29] In the same study, molecular modeling was used to demonstrate that the position of secondary amines in the polyamine region is important for key interactions with residues in the iGlu ion channel and that these interact differentially with NMDA and AMPA receptors, thus providing an opportunity for design of analogues of **2** with improved AMPA versus NMDA receptor selectivity. In the current work, we have explored this rationale by designing a range of derivatives of **2** and prepared these by the newly developed SPS methodology, exploiting first the role of secondary amines in the polyamine region in a systematic manner and subsequently examining the importance of the headgroup and linker amino acid region of these derivatives.

RESULTS AND DISCUSSION

Design and Synthesis. Initially, we wanted to examine the importance of the relative position of the secondary amino group in the polyamine moiety of the two ArgTX-636 derivatives previously synthesized and characterized, namely, ArgTX-93 and ArgTX-57, which are potent inhibitors and show about 32- and 11-fold selectivity of NMDA and AMPA receptors, respectively.[29] Thus, using an SPS methodology similar to what was previously described,[29] we systematically modified the relative position of the secondary amino group in the polyamine moiety, leading to seven derivatives, ArgTX-39 to ArgTX-93 (**3**−**9**, Scheme 1). These were synthesized, essentially as previously described. Briefly mononosyl protected diamines with three to nine methylene groups were loaded onto a backbone amide linker (BAL) by reductive amination (Scheme 1) followed by successive peptide couplings generating the headgroup to provide resin-bound intermediates **10**−**16** (Scheme 1). After liberation of a primary amino group, *N*-2-(trimethylsilyl)ethyloxycarbonyl (Teoc) protected amino alcohols were reacted with **10**−**16** in Fukuyama−Mitsunobu reactions, providing the polyamine moiety (**17**−**23**). The terminal protected arginine was then coupled followed by deprotection of nosyl-protected amines to provide resin-bound,

dx.doi.org/10.1021/jm301602d | J. Med. Chem. 2013, 56, 1171−1181

Scheme 2. Synthesis of Compounds 5a–h and 8a–h[a]

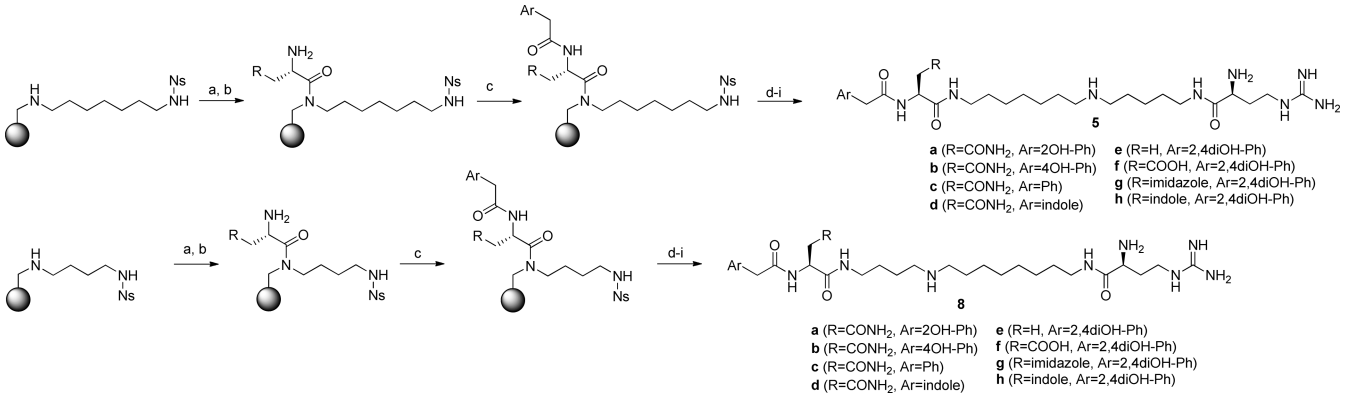

[a]Reagents and conditions: (a) Fmoc-L-Asn(Trt)-OH, Fmoc-L-Ala-OH, Fmoc-L-Asp(^{t}Bu)-OH, Fmoc-L-His(Trt)-OH, or Fmoc-L-Trp(Boc)-OH, HATU, DIPEA; (b) 20% piperidine in DMF; (c) 2-(2,4-bis(benzyloxy)phenyl)acetic acid, (2-benzyloxy)phenylacetic acid, (4-benzyloxy)-phenylacetic acid, phenylacetic acid, or 2-(1*H*-indol-3-yl)acetic acid, HATU, DIPEA; (d) *N*-Teoc amino alcohol, Bu_3P, ADDP; (e) TBAF, 55 °C; (f) Fmoc-L-Arg(Pbf)-OH, HATU, DIPEA; (g) DBU, 2-mercaptoethanol; (h) TFA/DCM/TIPS/H_2O (75:20:2.5:2.5); (i) H_2, $Pd(OH)_2$/C.

Table 1. Antagonist Effect of Argiotoxin Analogues 2–9 at AMPA and NMDA Receptors

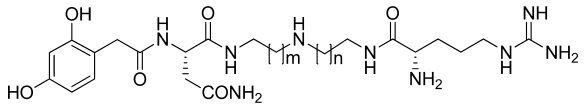

compd	*m*	*n*	IC_{50} (nM)[a] GluA1[b]	IC_{50} (nM)[a] GluN1/2A[c]	selectivity[d]
ArgTX-636 (**2**)			77 [62–95][e]	10 [9–11][e]	8
ArgTX-93 (**3**)	8	2	454 [282–428][e]	14 [13–16][e]	32
ArgTX-84 (**4**)	7	3	83 [73–94]	8 [7–10]	10
ArgTX-75 (**5**)	6	4	118 [100–139]	17 [14–21]	7
ArgTX-66 (**6**)	5	5	46 [41–52]	21 [19–25]	2
ArgTX-57 (**7**)	4	6	78 [67–90][e]	842 [735–963][e]	0.09 (11[f])
ArgTX-48 (**8**)	3	7	19 [17–22]	231 [195–274]	0.08 (12[f])
ArgTX-39 (**9**)	2	8	171 [29–227]	>3000	<0.06 (18[f])

[a]IC_{50} values determined from nonlinear regression fitting to a logistic equation of composite dose–response data obtained from 5 to 10 oocytes. Numbers in brackets denote the 95% confidence interval for IC_{50}. [b]Inhibition of the current elicited by 300 μM L-glutamate by simultaneous coapplication of the antagonist in oocytes injected with $GluA1_i$. [c]Inhibition of the current elicited by 100 μM L-glutamate and 100 μM glycine by simultaneous coapplication of the antagonist in oocytes injected with a 1:1 ratio of GluN1/N2A. [d]Selectivity ratio calculated as IC_{50}(GluA1)/IC_{50}(GluN1/2A). [e]Data from ref 29. [f]IC_{50}(GluN1/2A)/IC_{50}(GluA1).

protected ArgTX derivatives **24–30** (Scheme 1). Subsequent cleavage from the resin with concomitant cleavage of *N*-pentamethyl-2,3-dihydrobenzofuran-5-sulfonyl (Pbf), *N*-*tert*-butoxycarbonyl (Boc), and *N*-trityl (Trt) protecting groups provided bis-benzyl ArgTX derivatives. The seven target compounds **3–9** were obtained in moderate to good yields after removal of the *O*-benzyl protecting groups by treatment with H_2 and $Pd(OH)_2$/C.

The initial biological screening of these derivatives led us to select ArgTX-75 (**5**) and ArgTX-48 (**8**) for further structure–activity relationship (SAR) studies, and derivatives of **5** and **8** were therefore designed and synthesized. Knowing that the guanidinium moiety is essential for biological activity and having optimized the polyamine moiety, we next wanted to modify the headgroup and the linker amino acid, the 2,4-dihydroxyphenyl acetic acid and asparagine moiety, respectively. These changes were introduced in both **5** and **8** in order to systematically evaluate their importance for potency and selectivity at iGlu receptors. A synthetic route similar to that described above was used where mononosyl protected heptane-1,7-diamine or butane-1,4-diamine for derivatives of **5** or **8**, respectively, was linked to the resin followed by introduction of the modifications in the linker amino acid and the aromatic moiety (Scheme 2). First, the aromatic headgroup was modified; i.e., the 2,4-dihydroxyphenyl acetic acid moiety was systematically modified while the asparagine linker was kept constant. 2-Hydroxyphenylacetic acid, 4-hydroxyphenylacetic acid, and phenylacetic acid, together with 2-(1*H*-indol-3-yl)acetic acid, were introduced instead of 2,4-dihydroxyphenyl-acetic acid in both **5** and **8** (Scheme 2). For the derivatives with modifications in the linker amino acid, alanine, aspartate, histidine, and tryptophan were exchanged with the asparagine linker, while the 2,4-dihydroxyphenylacetic acid moiety was not changed. Subsequently, the polyamine chain was elongated by reaction with *N*-Teoc protected 5-aminopentan-1-ol or 8-aminooctan-1-ol for derivatives of **5** or **8**, respectively, and by application of the strategy described above, the 16 derivatives **5a–h** and **8a–h** were prepared (Scheme 2).

Pharmacology. The inhibitory potency of compounds **3–9**, **5a–h**, and **8a–h** was evaluated using two-electrode voltage-clamp (TEVC) electrophysiology with *Xenopus laevis* oocytes expressing the flip form of the homomeric AMPA receptor

dx.doi.org/10.1021/jm301602d | J. Med. Chem. 2013, 56, 1171–1181

Table 2. Antagonist Effect of Argiotoxin Analogues 5a–h at AMPA and NMDA Receptors

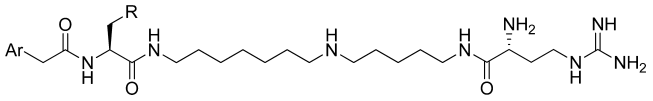

Cmpd.	Ar	R	IC_{50} (nM)[a] GluA1[b]	IC_{50} (nM)[a] GluN1/2A[c]	Selectivity[d]
ArgTX-75 (**5**)	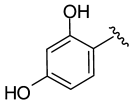	$CONH_2$	118 [100-139]	17 [14-21]	7
5a			77 [66-91]	122 [109-137]	0.6
5b	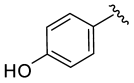		96 [85-109]	81 [73-91]	1.2
5c		$CONH_2$	124 [109-140]	165 [138-198]	0.8
5d	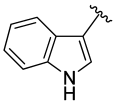		57 [53-61]	5 [4-5]	11
5e		H	105 [97-115]	103 [94-113]	1.0
5f		COOH	167 [156-178]	2230 [1980-2500]	0.07 (13[e])
5g	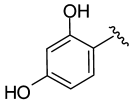	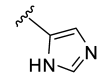	43 [38-48]	72 [64-81]	0.6
5h		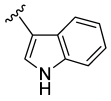	17 [15-19]	5 [4-5]	3.4

[a]IC_{50} values determined from nonlinear regression fitting to a logistic equation of composite dose–response data obtained from 5 to 10 oocytes. Numbers in brackets denote the 95% confidence interval for IC_{50}. [b]Inhibition of the current elicited by 300 μM L-glutamate by simultaneous coapplication of the antagonist in oocytes injected with $GluA1_i$. [c]Inhibition of the current elicited by 100 μM L-glutamate and 100 μM glycine by simultaneous coapplication of the antagonist in oocytes injected with a 1:1 ratio of GluN1/N2A. [d]Selectivity ratio calculated as IC_{50}(GluA1)/IC_{50}(GluN1/2A). [e]Selectivity ratio calculated as IC_{50}(GluN1/2A)/IC_{50}(GluA1).

subtype GluA1 or the heteromeric NMDA receptor subtype consisting of GluN1 and GluN2A subunits (Figure 2A). IC_{50} values for the inhibition by compounds **3**–**9** were determined at a membrane potential (V_H) of −40, −60, and −80 mV (Tables S1 and S2 and Table 1, respectively), while compounds **5a**–**h** and **8a**–**h** were tested at V_H of −60 and −80 mV (Tables S3 and 2, and Tables S4 and 3, respectively).

Inspired by the conversion of the nonselective iGlu receptor antagonist ArgTX-636 (**2**) into **3** and **7** with preference for NMDA and AMPA receptors, respectively,[29] we were interested in examining the importance of a systematic variation of the secondary amine of the polyamine tail for their inhibitory activity at AMPA and NMDA receptors. Thus, the seven compounds **3**–**9**, where the secondary amino group was sequentially moved from the N-terminal tail closer to the aromatic headgroup, were tested in the TEVC assay at V_H = −40 mV (Table S1), −60 mV (Table S2), and −80 mV (Table 1). In general, we observed a distinct correlation between the location of the secondary amino group and the preference for either AMPA or NMDA receptors. Compounds **3**, **4**, and **5** with the secondary amino group closest to the N-terminal tail showed a preference for NMDA receptors and displayed low nanomolar affinities for the NMDA receptor. Compound **6** was almost equally potent at AMPA and NMDA receptors, thus being nonselective, and generally showed affinities similar to that of the native toxin **2** (Table 1). On the other hand, when the secondary amino group was moved closer to the headgroup, as in compounds **7**, **8**, and **9**, affinities for AMPA receptors generally increase concomitantly with decreasing affinity for NMDA receptors, thus showing preference for AMPA receptors (Table 1). Gratifyingly, we saw that the potency at AMPA receptors was improved for compound **8** with an IC_{50} of 19 nM while displaying a 12-fold selectivity relative to NMDA receptors. Notably, **9** showed even improved selectivity for AMPA receptors compared to both **7** and **8**, which however was due to lack of inhibitory activity at NMDA rather than potent activity at AMPA receptors (Table 1). These observations correlate with previous modeling studies of **2** docked into models of the ion channels of AMPA and NMDA receptors, respectively.[29] These studies showed that the location of secondary amino groups is important both for internal hydrogen bonding in **2** and for interaction with key residues in the channel.[29]

Trends similar to those observed at V_H = −80 mV (Table 1) were also observed at V_H = −40 mV (Table S1) and −60 mV (Table S2). Moreover, from these data at the three holding

dx.doi.org/10.1021/jm301602d | J. Med. Chem. 2013, 56, 1171–1181

Table 3. Antagonist Effect of Argiotoxin Analogues 8a–h at AMPA and NMDA Receptors

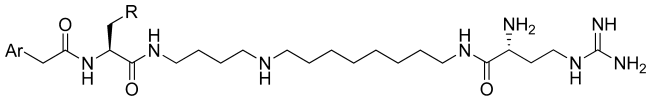

			IC_{50} (nM)[a]		
Cmpd.	Ar	R	GluA1[b]	GluN1/2A[c]	Selectivity[d]
ArgTX-48 (**8**)	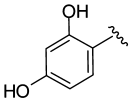	$CONH_2$	19 [17-22]	231 [195-274]	12
8a			37 [33-41]	2860 [2460-3100]	77
8b	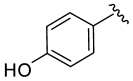		84 [77-93]	2320 [1950-2760]	28
8c		$CONH_2$	94 [83-107]	> 3000	>32
8d	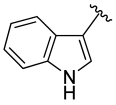		81 [74-89]	936 [853-1030]	12
8e		H	62 [53-72]	2060 [1590-2660]	33
8f		COOH	466 [409-532]	>3000	>6
8g	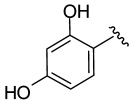	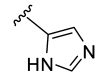	52 [45-60]	2090 [1760-2500]	40
8h		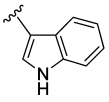	28 [25-32]	256 [225-290]	9

[a]IC_{50} values determined from nonlinear regression fitting to a logistic equation of composite dose–response data obtained from 5 to 10 oocytes. Numbers in brackets denote the 95% confidence interval for IC_{50}. [b]Inhibition of the current elicited by 300 μM L-glutamate by simultaneous coapplication of the antagonist in oocytes injected with $GluA1_i$. [c]Inhibition of the current elicited by 100 μM L-glutamate and 100 μM glycine by simultaneous coapplication of the antagonist in oocytes injected with a 1:1 ratio of GluN1/N2A. [d]Selectivity ratio calculated as IC_{50}(GluN1/2A)/IC_{50}(GluA1).

potentials we could estimate voltage dependency of the analogues responses, which generally confirmed that all compounds display voltage-dependent inhibition, as would be expected from ion channel blockers.[8] In conclusion, removal of a secondary amino group from the polyamine moiety of the native toxin **2** and systematic manipulation of the remaining secondary amino group showed a distinct correlation between location of this amino group and preference for either AMPA or NMDA receptors, and in some cases improvement in absolute potency was observed.

We have earlier shown that modifications of both polyamine moiety and headgroup of the prototypical polyamine toxin PhTX-433 (**1**) influence the inhibitory potency and selectivity,[17,18,20,22] and we have also seen for spider polyamine toxins that the headgroup in particular is highly important for selective inhibition of iGlu receptors.[26] Thus, having exploited systematic modifications of the polyamine moiety of **2** and knowing that changes in the tail amino acid, particularly modifying the guanidinium group of arginine, lead to substantial loss in inhibitory activity at both AMPA and NMDA receptors,[29] we focused on the importance of changes in the headgroup (2,4-dihydroxyphenylacetic acid) and linker amino acid (asparagine) region (Figure 1). We selected the two derivatives, **5** and **8**, that in our initial screening showed most promise and designed a set of derivatives where the same changes in the headgroup and linker amino acid were introduced into **5** and **8**, respectively (Scheme 2). Since we had no prior knowledge on the importance of changes in this region, we introduced subtle changes in the 2,4-dihydroxyphenylacetic acid moiety, as well as more drastic modifications of the asparagine amino acid linker, and a total of 16 analogues of **5** and **8** were prepared.

First, we looked into the importance of the number and position of headgroup hydroxyl groups by substituting the 2,4-dihydroxyphenylacetic acid moiety with 2-hydroxyphenylacetic acid, 4-hydroxyphenylacetic acid, and phenylacetic acid. Finally, we also substituted the 2,4-dihydroxyphenylacetic acid moiety with a 2-(1*H*-indol-3-yl)acetic acid because a range of structurally similar spider toxins, such as *Nephila* polyamine toxin-8 (NPTX-8),[24,26] contain this indole moiety as the headgroup. Next, we tested the consequence of substituting the amino acid linker asparagine, choosing four different amino acids (alanine, aspartic acid, histidine, and tryptophan) with alkyl, carboxylic acid, or aromatic side chains. These modifications were conveniently introduced using the same SPS methodology as described above (Scheme 2).

dx.doi.org/10.1021/jm301602d | J. Med. Chem. 2013, 56, 1171–1181

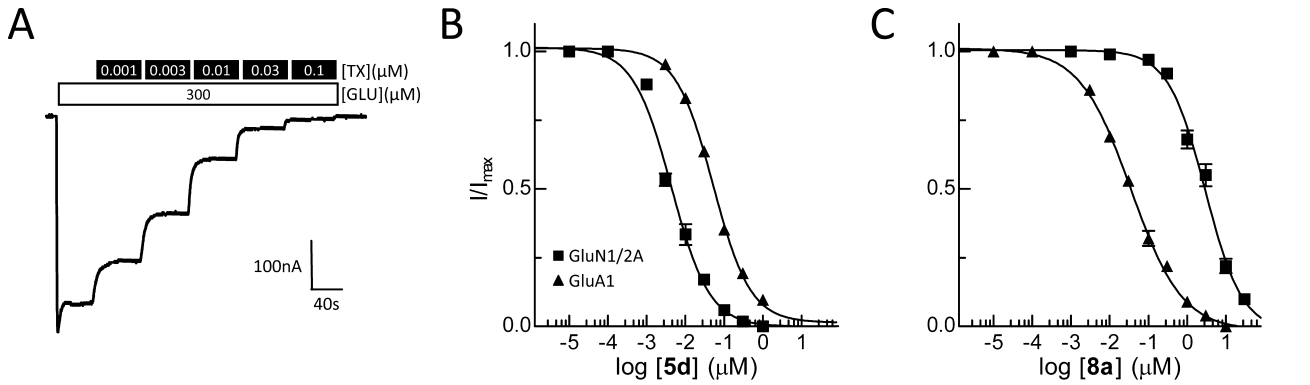

Figure 2. Inhibitory potency of toxins at recombinant iGlu receptor subtypes. (A) Representative two-electrode voltage-clamp current recording illustrating the standard testing protocol. Oocytes expressing iGlu receptor were exposed to maximally effective concentrations of agonist, followed by increasing concentrations of the test toxin plus agonist (B, C). Composite concentration−response curves for **5d**, in which the headgroup of **5** has been replaced with 2-(1*H*-indol-3-yl)acetic acid (B), and for **8a**, in which the headgroup of **8** has been replaced with 2-hydroxyphenylacetic acid (C) at GluN1/2A (■) and GluA1 (▲) receptors at membrane potentials of −80 mV. Error bars are SEM and are shown when larger than symbol size.

Modification of the position and number of headgroup hydroxyl groups of **5**, with preference for the NMDA receptor, generally reduced potency at NMDA receptors as observed for compounds **5a−c**, whereas potency at AMPA receptors was largely unaffected. The selectivity profile of **5a−c** was thereby changed to largely nonselective inhibitors (Table 2). In contrast, when an indole headgroup is introduced, as in **5d**, potency at NMDA receptors was improved with an IC_{50} of 5 nM whereas potency at AMPA receptors was improved only about 2-fold, thereby slightly improving the selectivity relative to **5** (Figure 2B). The most pronounced effect observed at NMDA receptors was obtained by substituting the amino acid linker asparagine with aspartic acid (**5f**), which resulted in a 131-fold loss of potency, while potency at AMPA receptors was largely unaffected, thereby shifting the preference to AMPA receptors. Substitution with alanine (**5e**) resulted in a 5-fold loss of potency at NMDA receptors, whereas AMPA receptor potency was not affected. Replacing the asparagine linker with histidine (**5g**) improved potency at AMPA receptors slightly, while the reverse was true for NMDA receptor potency. Notably, introducing a tryptophan (**5h**), i.e., introducing an indole group similar to **5d**, resulted in significant improvement of potency at both NMDA and AMPA receptors with IC_{50} values of 5 and 17 nM, respectively (Table 2). Thus, changes in the headgroup and linker amino acid region of **5** led to identification of **5d** and **5h** both having IC_{50} of 5 nM at NMDA receptors, and **5d** showed improved selectivity compared to **5**. Interestingly, both **5d** and **5h** contain an indole moiety in either the headgroup or linker amino acid, suggesting that such a moiety is particularly useful in improving NMDA receptor potency. A similar observation that an indole headgroup improved potency at iGlu receptors was recently found for structurally related compounds, the *Nephila* polyamine toxins.[26]

We also evaluated the biological consequences of introducing the same changes into the headgroup and linker amino acid region of the AMPA receptor, preferring compound **8** (Table 3). Modifications of the hydroxylation pattern of the 2,4-dihydroxyphenylacetic acid moiety of **8**, compounds **8a−c**, as well as substitution with an indole (**8d**), had only minor effect on potency at AMPA receptors with IC_{50} values from 37 to 94 nM (Table 3). In contrast, the effect on NMDA receptor potency was much more drastic, as significant reductions were observed for all analogues, and hence, the selectivity for AMPA receptors was drastically improved, and **8a** (Figure 2C) and **8c** showed 77-fold and >32-fold selectivity, respectively, for AMPA vs NMDA receptors. Replacing the asparagine linker showed similar tendencies; AMPA receptor potency was not much affected except when substituting with aspartic acid (**8f**), while potency at NMDA receptors was dramatically reduced except for introduction of tryptophan (**8h**) (Table 3).

In order to get an estimate of the voltage dependency, which is a hallmark of this class of inhibitors, we also tested compounds **5a−h** and **8a−h** at a holding potential (V_H) of −60 mV (Tables S3 and S4). Generally, we observed that all analogues were less potent at V_H = −60 mV compared to IC_{50} measured at V_H = −80 mV, as would be expected from voltage-dependent inhibitors. This suggests that all the investigated compounds still act as voltage-dependent channel blockers of AMPA and NMDA receptors.

■ CONCLUSION

We have used ArgTX-636 (**2**) as a template for the development of potent and selective iGlu receptor ligands and have performed the first SAR study of spider polyamine toxins in general and **2** in particular. A recently developed solid-phase synthesis methodology was exploited for the synthesis of two classes of analogues: first, there is the importance of secondary amines of the polyamine moiety, and second, the headgroup and linker amino acid were systematically examined and evaluated for activity at AMPA and NMDA receptors. For the first class of analogues, compounds **3−9**, we observed a distinct correlation between the location of the secondary amino group in the polyamine moiety and inhibition of AMPA and NMDA receptors: if the amino group was closer to the headgroup, compounds showed preference for NMDA receptors, whereas if the amino group was closer to the amino acid tail, preference for AMPA receptors was observed. Two analogues, **5** and **8**, were selected for further derivatization in the headgroup and linker amino acid region. The two regions had not been previously investigated for argiotoxin analogues. Changes in these two regions generally had more pronounced biological effect than those in the polyamine region. For analogues of **5** it was observed that highly potent and reasonable NMDA receptor selective ligands could be developed by introducing indole moieties, exemplified with compound **5d**. On the other hand, introducing the same modifications in **8** led to fairly potent and highly selective AMPA receptors ligands such as **8a**. Thus, exploiting SAR

dx.doi.org/10.1021/jm301602d | *J. Med. Chem.* 2013, 56, 1171−1181

studies of spider polyamine toxins clearly provides a useful and efficient way to develop notable tools for studies of iGlu receptors.

EXPERIMENTAL SECTION

Chemistry. General Procedures. Unless otherwise stated, starting materials were obtained from commercial suppliers and were used without further purification. 2-(3,5-Dimethoxy-4-formylphenoxy)ethylpolystyrene with a loading of 0.92 mmol/g was purchased from Novabiochem. *N*-(Aminoalkyl)-2-nitrobenzenesulfonamide, *N*-(trimethylsilyl)ethoxycarbonylamino alcohols, 2-(2,4-bis(benzyloxy)phenyl)acetic acid, (2-benzyloxy)phenylacetic acid, and (4-benzyloxy)phenylacetic acid were prepared as previously described.[20] Tetrahydrofuran (THF) was distilled under nitrogen from sodium/benzophenone immediately before use. *N*,*N*-Dimethylformamide (DMF) and dichloromethane were dried using AldraAmine trapping packets. Proton (^{1}H) NMR spectra were recorded on a Varian spectrometer, Mercury Plus (300 MHz), and carbon (^{13}C) NMR spectra were recorded on a Varian spectrometer, Gemini 2000 (75 MHz). Chemical shifts (δ) are reported in parts per million (ppm) with reference to tetramethylsilane (TMS) as internal standard. The following abbreviations are used for the proton spectra multiplicities: s, singlet; bs, broad singlet; d, doublet; dd, double doublet, t, triplet; q, quartet; m, multiplet. Coupling constants (J) are reported in hertz (Hz). Preparative HPLC was performed on a Agilent 1100 system using a C18 reverse phase column (Zorbax 300 SB-C18, 21.2 mm × 250 mm) with a linear gradient of the binary solvent system of H_2O/ACN/TFA (A, 95/5/0.1; B, 5/95/0.1) with a flow rate of 20 mL/min. Analytical HPLC was performed on an Agilent 1100 system with a C18 reverse phase column (Zorbax 300 SB-C18 column, 4.6 mm × 150 mm), flow rate of 1 mL/min, and a linear gradient of the binary solvent system of H_2O/ACN/TFA (A, 95/5/0.1; B, 5/95/0.1). Mass spectra were obtained with an Agilent 6410 triple quadrupole mass spectrometer instrument using electron spray coupled to an Agilent 1200 HPLC system (ESI-LC/MS) with a C18 reverse phase column (Zorbax Eclipse XBD-C18, 4.6 mm × 50 mm), autosampler, and diode array detector using a linear gradient of the binary solvent system of H_2O/ACN/formic acid (A, 95/5/0.1; B, 5/95/0.086) with a flow rate of 1 mL/min. During ESI-LC/MS analysis evaporative light scattering (ELS) traces were obtained with a Sedere Sedex 85 light scattering detector. Compound identity of all tested compounds was confirmed by ESI-LC/MS, which also provided purity data (all >95%, UV and ELSD). High-resolution mass spectra were obtained using a Micromass Q-Tof II instrument, and results were all within ±5 ppm of theoretical values.

General Synthetic Procedure A. Compounds 2−9. 2-(3,5-Dimethoxy-4-formylphenoxy)ethylpolystyrene resin (0.45 mmol) was treated with a solution of *N*-(aminoalkyl)-2-nitrobenzenesulfonamide (4.50 mmol) in DMF/acetic acid (9:1, 16 mL). The reaction mixture was agitated for 2 min, and $NaBH(OAc)_3$ (4.50 mmol) was added in one portion. The mixture was agitated for 12 h at room temperature. The solvents were drained, and the resin was washed with DMF, DIPEA (10% in DMF), DMF, CH_2Cl_2, MeOH, CH_2Cl_2 (3 × 16 mL each) and dried in a vacuum. A solution of Fmoc-L-Asn(Trt)-OH (2.25 mmol) and HATU (2.25 mmol) in CH_2Cl_2/DMF (9:1, 16 mL) was added to the above resin followed by DIPEA (4.50 mmol). The mixture was agitated for 12 h, and the resin was subsequently washed with DMF, CH_2Cl_2, MeOH, CH_2Cl_2 (3 × 16 mL each) and dried under reduced pressure. The product was treated with 20% piperidine in DMF (v/v, 16 mL) and the mixture agitated for 2 min at room temperature. The resulting resin was washed with DMF (3 × 16 mL), treated again with 20% piperidine in DMF (v/v, 16 mL) for 20 min, and then washed with DMF, CH_2Cl_2, MeOH, and CH_2Cl_2 (3 × 16 mL each). This resin was treated with a solution of 2-(2,4-bis(benzyloxy)phenyl)acetic acid (2.25 mmol) and HATU (2.25 mmol) in CH_2Cl_2/DMF (9:1, 16 mL), followed by DIPEA (4.50 mmol). The mixture was agitated for 2 h at room temperature and subsequently drained and washed with DMF, DCM, MeOH, and DCM (3 × 16 mL each). The above resin was suspended in dry THF/CH_2Cl_2 (1:1, 6 mL) under nitrogen. A solution of a *N*-Teoc amino alcohol (2.25 mmol) in dry THF/CH_2Cl_2 (1:1, 3 mL), tributylphosphine (2.25 mmol), and a solution of 1,1′-(azadicarbonyl)dipiperidine (ADDP, 2.25 mmol) in dry THF/CH_2Cl_2 (1:1, 3 mL) were added successively. The mixture was stirred at room temperature under nitrogen for 3 h. The resin was drained and washed with DMF, CH_2Cl_2, MeOH, and CH_2Cl_2 (3 × 16 mL each) and dried in a vacuum. The procedure was repeated two more times, and the resulting resin was dried in a vacuum. The above resin was suspended in dry THF (16 mL) under nitrogen at 50 °C. A solution of TBAF (1 M in THF, 1.80 mmol) was added slowly, and the mixture was stirred at 50 °C for 30 min. The resin was drained and washed with DMF, CH_2Cl_2, MeOH, and CH_2Cl_2 (3 × 16 mL each) and dried in a vacuum. The resin was then treated with a solution of Boc-L-Arg(Pbf)-OH (2.25 mmol) and HATU (2.25 mmol) in CH_2Cl_2/DMF (9:1, 16 mL), followed by DIPEA (4.50 mmol), and agitated for 2 h at room temperature and subsequently drained and washed with DMF, CH_2Cl_2, MeOH, and CH_2Cl_2 (3 × 16 mL each). The resin was treated with DBU (1.80 mmol) in DMF (6 mL) and mercaptoethanol (1.80 mmol) in DMF (6 mL) for 30 min. The resin was drained and washed with DMF (5 × 12 mL). The procedure was repeated three more times. The resin was washed with DMF, CH_2Cl_2, MeOH, and CH_2Cl_2 (3 × 16 mL each) and then treated with a solution of TFA/CH_2Cl_2/triisopropylsilane/H_2O (75:20:2.5:2.5 v/v/v/v, 12 mL) for 2 h. The resin was drained and washed with MeOH (6 mL) and CH_2Cl_2 (6 mL). The solutions of the cleaved product and the washings were combined and evaporated in a vacuum and purified by preparative HPLC. A screw cap vial was charged with a magnetic stir bar and the bis-benzyl protected argiotoxin derivative followed by glacial acetic acid (4 mL). $Pd(OH)_2$/C (10% w/w) was added and the vial sealed with a rubber septum. Hydrogen was bubbled through the solution for about 30 min. The mixture was filtered with a 0.2 μm syringe filter and washed several times with MeOH. The combined washings were concentrated in vacuo to give an off-white solid which was purified by preparative HPLC and lyophilized to give the argiotoxin derivative as a fluffy white solid. Compounds **2**, **3**, and **7** were prepared previously.[20]

(*S*)-*N*^{1}-(8-(4-((*S*)-2-Amino-5-guanidinopentanamido)-butylamino)octyl)-2-(2-(2,4-dihydroxyphenyl)acetamido)-succinamide Tris(2,2,2-trifluoroacetate (ArgTX-84, 4). Yield: 64.5 mg (14.7%). ^{1}H NMR (300 MHz, CD_3OD): δ = 6.93 (d, J = 8.3 Hz, 1H), 6.34 (d, J = 2.5 Hz, 1H), 6.28 (dd, J = 8.3, 2.5 Hz, 1H), 4.66 (t, J = 6.3 Hz, 1H), 3.87 (t, J = 6.6 Hz, 1H), 3.50 (d, J = 14.9 Hz, 1H), 3.41 (d, J = 14.9 Hz, 1H), 3.21−3.29 (m, 4H), 2.90−3.14 (m, 6H), 2.69 (d, J = 6.3 Hz, 2H), 1.90 (m, 2H), 1.59−1.74 (m, 8H), 1.46 (m, 2H), 1.25−1.35 (m, 8H). ^{13}C NMR (75 MHz, CD_3OD): δ = 175.1, 174.0, 173.0, 169.9, 159.1, 158.7, 157.3, 132.8, 114.2, 108.1, 103.9, 54.3, 52.0, 41.9, 40.5, 40.0, 38.9, 37.6, 30.2, 30.0, 29.8, 29.8, 27.5, 27.3, 27.2, 27.2, 25.7, 24.8. HPLC-ELS: 100%. m/z = 636.5 [MH$^+$]. HRMS (EI) exact mass calculated for $C_{30}H_{53}N_9O_6$ [MH$^+$] 636.4197. Found: 636.4194.

(*S*)-*N*^{1}-(7-(5-((*S*)-2-Amino-5-guanidinopentanamido)-pentylamino)heptyl)-2-(2-(2,4-dihydroxyphenyl)acetamido)-succinamide Tris(2,2,2-trifluoroacetate (ArgTX-75, 5). Yield: 24.3 mg (5.5%). ^{1}H NMR (300 MHz, CD_3OD): δ = 6.93 (d, J = 8.3 Hz, 1H), 6.33 (d, J = 2.2 Hz, 1H), 6.26 (dd, J = 8.3, 2.5 Hz, 1H), 4.64 (t, J = 6.3 Hz, 1H), 3.84 (t, J = 6.6 Hz, 1H), 3.51 (d, J = 15.1 Hz, 1H), 3.40 (d, J = 15.1 Hz, 1H), 3.19−3.26 (m, 4H), 3.09 (m, 2H), 2.84−2.96 (m, 4H), 2.69 (d, J = 6.6 Hz, 2H), 1.88 (m, 2H), 1.53−1.69 (m, 8H), 1.38−1.47 (m, 4H), 1.24−1.35 (m, 6H). ^{13}C NMR (75 MHz, CD_3OD): δ = 175.2, 175.0, 173.1, 169.8, 159.1, 158.7, 157.3, 132.9, 114.3, 108.1, 103.9, 54.2, 52.0, 41.9, 40.4, 40.3, 38.9, 37.4, 30.0, 30.0, 30.0, 29.2, 27.0, 27.0, 26.9, 26.7, 25.7, 25.0. HPLC-ELS: 100%. m/z = 636.4 [MH$^+$]. HRMS (EI) exact mass calculated for $C_{30}H_{53}N_9O_6$ [MH$^+$] 636.4197. Found: 636.4193.

(*S*)-*N*^{1}-(6-(6-((*S*)-2-Amino-5-guanidinopentanamido)-hexylamino)hexyl)-2-(2-(2,4-dihydroxyphenyl)acetamido)-succinamide Tris(2,2,2-trifluoroacetate (ArgTX-66, 6). Yield: 26.3 mg (6.0%). ^{1}H NMR (300 MHz, CD_3OD): δ = 6.93 (d, J = 8.0 Hz, 1H), 6.33 (d, J = 2.5 Hz, 1H), 6.26 (dd, J = 8.0, 2.5 Hz, 1H), 4.62 (t, J = 6.6 Hz, 1H), 3.84 (t, J = 6.6 Hz, 1H), 3.50 (d, J = 15.1 Hz, 1H),

dx.doi.org/10.1021/jm301602d | J. Med. Chem. 2013, 56, 1171−1181

3.40 (d, J = 15.1 Hz, 1H), 3.09−3.26 (m, 6H), 2.92 (t, J = 7.7 Hz, 2H), 2.86 (t, J = 7.9 Hz, 2H), 2.69 (m, 2H), 1.88 (m, 2H), 1.61−1.71 (m, 4H), 1.53−1.60 (m, 4H), 1.46 (m, 2H), 1.37−1.42 (m, 4H), 1.26−1.33 (m, 4H). ^{13}C NMR (75 MHz, CD_3OD): δ = 175.1, 175.0, 173.1, 169.7, 159.1, 158.6, 157.3, 132.9, 114.3, 108.1, 103.9, 54.2, 52.0, 49.0, 48.8, 41.9, 40.7, 40.3, 39.0, 37.4, 30.2, 30.0, 30.0, 27.6, 27.3, 27.1, 27.1, 27.0, 27.0, 25.7. HPLC-ELS: 100%. m/z = 636.4 [MH$^+$]. HRMS (EI) exact mass calculated for $C_{30}H_{53}N_9O_6$ [MH$^+$] 636.4197. Found: 636.4176.

(*S*)-*N*^{1}-(4-(8-((*S*)-2-Amino-5-guanidinopentanamido)-nonylamino)propyl)-2-(2-(2,4-dihydroxyphenyl)acetamido)-succinamide Tris(2,2,2-trifluoroacetate (ArgTX-48, 8). Yield: 76.8 mg (17.5%). ^{1}H NMR (300 MHz, CD_3OD): δ = 6.94 (d, J = 8.3 Hz, 1H), 6.35 (d, J = 2.2 Hz, 1H), 6.28 (dd, J = 8.3, 2.2 Hz, 1H), 4.61 (t, J = 6.3 Hz, 1H), 3.86 (t, J = 6.6 Hz, 1H), 3.51 (d, J = 15.1 Hz, 1H), 3.42 (d, J = 15.1 Hz, 1H), 3.20−3.26 (m, 6H), 2.87−2.92 (m, 4H), 2.71 (m, 2H), 1.89 (m, 2H), 1.55−1.72 (m, 10H), 1.34−1.38 (m, 8H). ^{13}C NMR (75 MHz, CD_3OD): δ = 175.2, 175.0, 173.3, 169.7, 159.0, 158.7, 157.2, 132.9, 114.2, 108.1, 103.9, 54.2, 52.1, 49.0, 41.8, 40.8, 39.4, 38.9, 37.4, 30.4, 30.2, 29.9, 28.0, 27.6, 27.4, 27.3, 25.6, 24.2. HPLC-ELS: 100%. m/z = 636.5 [MH$^+$]. HRMS (EI) exact mass calculated for $C_{30}H_{53}N_9O_6$ [MH$^+$] 636.4197. Found: 636.4190.

(*S*)-*N*^{1}-(3-(9-((*S*)-2-Amino-5-guanidinopentanamido)-nonylamino)propyl)-2-(2-(2,4-dihydroxyphenyl)acetamido)-succinamide Tris(2,2,2-trifluoroacetate (ArgTX-39, 9). Yield: 22.8 mg (5.2%). ^{1}H NMR (300 MHz, CD_3OD): δ = 6.93 (d, J = 8.3 Hz, 1H), 6.32 (d, J = 2.5 Hz, 1H), 6.25 (dd, J = 8.3, 2.5 Hz, 1H), 4.57 (t, J = 5.8 Hz, 1H), 3.83 (t, J = 6.6 Hz, 1H), 3.45 (s, 2H), 3.32 (m, 2H), 3.24−3.18 (m, 4H), 2.90 (t, J = 7.2 Hz, 2H), 2.86−2.65 (m, 4H), 1.92−1.77 (m, 4H), 1.70−1.58 (m, 4H), 1.53 (t, J = 6.3 Hz, 2H), 1.39−1.33 (m, 10H). ^{13}C NMR (75 MHz, CD_3OD): δ = 175.4, 174.9, 174.6, 169.7, 159.1, 158.7, 157.2, 132.9, 114.2, 108.1, 103.8, 54.2, 52.0, 49.3, 46.2, 41.9, 40.9, 38.9, 37.2, 36.9, 30.6, 30.5, 30.5, 30.4, 30.0, 28.2, 27.7, 27.7, 27.6, 25.7. HPLC-ELS: 100%. m/z = 636.5 [MH$^+$]. HRMS (EI) exact mass calculated for $C_{30}H_{53}N_9O_6$ [MH$^+$] 636.4197. Found: 636.4183.

General Synthetic Procedure B. Compounds 5a−h and 8a−h. Compounds were prepared according to the general synthetic procedure A with the following exceptions. For compounds **5a−d** and **8a−d** the use of 2-(2,4-bis(benzyloxy)phenyl)acetic acid was replaced with (2-benzyloxy)phenylacetic acid (**a**), (4-benzyloxy)phenylacetic acid (**b**), phenylacetic acid (**c**), or 2-(1*H*-indol-3-yl)acetic acid (**d**), and when the last two compounds were employed the debenzylation step was avoided. For compounds **5e−h** and **8e−h**, the use of Fmoc-L-Asn(Trt)-OH was replaced with the use of Fmoc-L-Ala-OH (**e**), Fmoc-L-Asp(^{t}Bu)-OH (**f**), Fmoc-L-His(Trt)-OH (**g**), and Fmoc-L-Trp(Boc)-OH (**h**).

(*S*)-*N*^{1}-(7-((5-((*S*)-2-Amino-5-guanidinopentanamido)pentyl)-amino)heptyl)-2-(2-(2-hydroxyphenyl)acetamido)succinamide Tris(2,2,2-trifluoroacetate (5a). Yield: 42.1 mg (14.6%). ^{1}H NMR (300 MHz, CD_3OD): δ = 7.03−7.15 (m, 2H), 6.72−6.84 (m, 2H), 4.64 (t, J = 6.0 Hz, 1H), 3.84 (t, J = 6.4 Hz, 1H), 3.60 (d, J = 14.0 Hz, 1H), 3.49 (d, J = 15.0 Hz, 1H), 3.16−3.25 (m, 4H), 3.00−3.15 (m, 2H), 2.76−2.97 (m, 4H), 2.68 (d, J = 6.0, 2H), 1.75−1.96 (m, 2H), 1.59−1.72 (m, 4H), 1.49−1.59 (m, 4H), 1.36−1.48 (m, 4H), 1.22−1.32 (m, 6H). ^{13}C NMR (75 MHz, CD_3OD): δ = 174.9, 174.6, 173.0, 169.8, 158.7, 156.5, 132.4, 129.7, 123.3, 121.1, 116.4, 54.2, 52.1, 41.8, 40.5, 40.4, 39.5, 37.6, 30.1, 29.9, 29.3, 27.0, 26.8, 25.6, 25.0. HPLC-ELS: 100%. m/z = 620.4 [MH$^+$]. HRMS (EI) exact mass calculated for $C_{30}H_{53}N_9O_5$ [MH$^+$] 620.4248. Found: 620.4240.

(*S*)-*N*^{1}-(7-((5-((*S*)-2-Amino-5-guanidinopentanamido)pentyl)-amino)heptyl)-2-(2-(4-hydroxyphenyl)acetamido)succinamide Tris(2,2,2-trifluoroacetate (5b). Yield: 16.5 mg (5.7%). ^{1}H NMR (300 MHz, CD_3OD): δ = 7.10 (d, J = 8.3 Hz, 2H), 6.72 (d, J = 8.3 Hz, 2H), 4.65 (t, J = 5.8 Hz, 1H), 3.86 (t, J = 6.3 Hz, 1H), 3.47 (s, 2H), 3.11−3.28 (m, 6H), 2.90−3.00 (m, 4H), 2.56−2.75 (m, 2H), 1.52−1.74 (m, 8H), 1.40−1.51 (m, 4H), 1.24−1.40 (m, 6H). ^{13}C NMR (75 MHz, CD_3OD): δ = 174.7, 174.6, 173.0, 169.8, 158.7, 157.5, 131.3, 127.3, 116.4, 54.2, 52.1, 42.9, 42.0, 41.9, 40.4, 37.9, 30.1, 29.9, 29.5, 27.2, 27.0, 25.7, 25.0. HPLC-ELS: 97%. m/z = 620.4 [MH$^+$]. HRMS (EI) exact mass calculated for $C_{30}H_{53}N_9O_5$ [MH$^+$] 620.4248. Found: 620.4226.

(*S*)-*N*^{1}-(7-((5-((*S*)-2-Amino-5-guanidinopentanamido)pentyl)-amino)heptyl)-2-(2-phenylacetamido)succinamide Tris(2,2,2-trifluoroacetate (5c). Yield: 13.4 mg (4.7%). ^{1}H NMR (300 MHz, CD_3OD): δ = 7.17−7.31 (m, 5H), 4.65 (t, J = 6.8 Hz, 1H), 3.84 (t, J = 6.4 Hz, 1H), 3.56 (s, 2H), 3.13−3.26 (m, 6H), 2.91−2.99 (m, 4H), 2.58−2.76 (m, 2H), 1.80−1.97 (m, 2H), 1.57−1.73 (m, 8H), 1.40−1.53 (m, 4H), 1.29−1.39 (m, 6H). ^{13}C NMR (75 MHz, CD_3OD): δ = 174.7, 174.0, 173.0, 169.8, 158.7, 136.7, 130.3, 130.2, 129.7, 129.6, 128.0, 54.2, 52.1, 43.7, 41.9, 40.4, 38.0, 30.1, 29.9, 29.6, 29.5, 27.4, 27.3, 27.1, 27.0, 25.7, 25.0. HPLC-ELS: 98%. m/z = 604.4 [MH$^+$]. HRMS (EI) exact mass calculated for $C_{30}H_{53}N_9O_4$ [MH$^+$] 604.4299. Found: 604.4277.

2-(2-(1*H*-Indol-3-yl)acetamido)-*N*^{1}-(7-(5-(2-amino-5-guanidinopentanamido)pentylamino)heptyl)succinamide Tetrakis(2,2,2-trifluoroacetate (5d). Yield: 14.1 mg (4.3%). ^{1}H NMR (300 MHz, CD_3OD): δ = 7.53 (d, J = 8.0 Hz, 1 H), 7.35 (d, J = 8.3 Hz, 1 H), 7.19 (s, 1 H), 7.10 (t, J = 7.5 Hz, 1 H), 7.01 (t, J = 7.4 Hz, 1 H), 4.67 (t, J = 7.6 Hz, 1 H), 3.84 (t, J = 7.4 Hz, 1 H), 3.73 (s, 2 H), 3.21 (t, J = 7.2 Hz, 4 H), 3.13−3.02 (m, 2 H), 2.92−2.70 (m, 4 H), 2.65 (d, J = 5.8 Hz, 2 H), 1.98−1.77 (m, 2 H), 1.72−1.47 (m, 9 H), 1.43−1.14 (m, 16 H). ^{13}C NMR (75 MHz, CD_3OD): δ = 173.8, 173.7, 171.9, 168.7, 137.1, 127.4, 124.1, 121.7, 119.1, 118.3, 111.5, 108.2, 53.2, 51.0, 40.8, 39.4, 39.2, 36.7, 33.0, 28.9, 28.9, 28.2, 28.2, 25.9, 25.9, 25.8, 25.7, 24.6, 23.9, 21.4. HPLC-ELS: 99%. m/z = 643.5 [MH$^+$]. HRMS (EI) exact mass calculated for $C_{32}H_{54}N_{10}O_4$ [MH$^+$] 643.4408. Found: 643.4401.

(*S*)-2-Amino-*N*-(5-((7-((*S*)-2-(2-(2,4-Dihydroxyphenyl)-acetamido)propanamido)heptyl)amino)pentyl)-5-guanidino-pentanamide Tris(2,2,2-trifluoroacetate (5e). Yield: 49.6 mg (17.7%). ^{1}H NMR (300 MHz, CD_3OD): δ = 6.88 (d, J = 7.3 Hz, 1H), 6.29 (s, 1H), 6.23 (d, J = 8.0 Hz, 1H), 4.21 (q, J = 7.0 Hz, 1H), 3.82 (t, J = 6.4 Hz, 1H), 3.47 (d, J = 14.7 Hz, 1H), 3.35 (d, J = 15.7 Hz, 1H), 2.98−3.24 (m, 6H), 2.77−2.95 (m, 4H), 1.75−1.94 (m, 2H), 1.59−1.71 (m, 4H), 1,47−1.58 (m, 4H), 1.33−1.46 (m, 4H), 1.20−1.33 (m, 9H). ^{13}C NMR (75 MHz, CD_3OD): δ = 175.1, 175.0, 169.8, 158.9, 158.7, 157.4, 132.8, 114.5, 108.0, 103.9, 54.2, 51.0, 49.0, 41.8, 40.4, 40.3, 38.7, 30.1, 29.9, 29.9, 29.4, 27.1, 27.0, 26.8, 25.7, 25.0, 18.1. HPLC-ELS: 100%. m/z = 593.4 [MH$^+$]. HRMS (EI) exact mass calculated for $C_{29}H_{52}N_8O_5$ [MH$^+$] 593.4139. Found: 593.4137.

(6*S*,24*S*)-1,6-Diamino-24-(2-(2,4-dihydroxyphenyl)-acetamido)-1-imino-7,23dioxo-2,8,14,22-tetraazahexacosan-26-oic Acid Tris(2,2,2-trifluoroacetate (5f). Yield: 36.6 mg (12.5%). ^{1}H NMR (300 MHz, CD_3OD): δ = 6.90 (d, J = 8.0 Hz, 1H), 6.31 (d, J = 1.9 Hz, 1H), 6.24 (dd, J = 1.9, 8.3 Hz, 1H), 4.62 (t, J = 6.3 Hz, 1H), 3.83 (t, J = 6.3 Hz, 1H), 3.48 (d, J = 14.9 Hz, 1H), 3.37 (d, J = 14.9 Hz, 1H), 3.01−3.25 (m, 6H), 2.79−2.95 (m, 4H), 2.70−2.78 (m, 2H), 1.77−1.93 (m, 2H), 1,48−1.72 (m, 8H), 1.33−1.47 (m, 4H), 1.20−1.32 (m, 6H). ^{13}C NMR (75 MHz, CD_3OD): δ = 175.3, 174.1, 172.9, 169.8, 159.0, 158.7, 157.3, 132.8, 114.3, 108.1, 103.9, 54.2, 51.7, 49.0, 41.9, 40.4, 38.9, 36.6, 30.1, 30.0, 29.9, 29.3, 27.1, 27.0, 26.8, 25.7, 25.0. HPLC-ELS: 100%. m/z = 637.4 [MH$^+$]. HRMS (EI) exact mass calculated for $C_{30}H_{52}N_8O_7$ [MH$^+$] 637.4037. Found: 637.4026.

(*S*)-2-Amino-*N*-(5-((7-((*S*)-2-(2-(2,4-dihydroxyphenyl)-acetamido)-3-(1*H*-imidazol-5-yl)propanamido)heptyl)amino)-pentyl-5-guanidinopentanamide Tetrakis(2,2,2-trifluoroacetate (5g). Yield: 31.6 mg (9.4%). ^{1}H NMR (300 MHz, CD_3OD): δ = 8.69 (s, 1H), 7.12 (s, 1H), 6.84 (d, J = 8.0 Hz, 1H), 6.29 (d, J = 2.2 Hz, 1H), 6.23 (dd, J = 2.2, 8.3 Hz, 1H), 4.61 (q, J = 5.0 Hz, 1H), 3.83 (t, J = 6.6 Hz, 1H), 3.38 (s, 2H), 3.14−3.23 (m, 6H), 2.85−3.06 (m, 6H), 1.79−1.95 (m, 2H), 1.52−1.69 (m, 8H), 1.36−1.49 (m, 4H), 1.25−1.35 (m, 6H). ^{13}C NMR (75 MHz, CD_3OD): δ = 175.3, 171.9, 169.8, 159.0, 158.7, 157.2, 134.8, 132.7, 131.2, 118.3, 114.2, 108.0, 103.9, 54.2, 53.7, 41.9, 40.6, 40.4, 38.7, 30.2, 30.0, 29.8, 28.2, 27.5, 27.4, 27.2, 27.0, 25.7, 25.0. HPLC-ELS: 100%. m/z = 659.4 [MH$^+$]. HRMS (EI) exact mass calculated for $C_{32}H_{54}N_{10}O_5$ [MH$^+$] 659.4357. Found: 659.4355.

(*S*)-2-Amino-*N*-(5-(7-((*S*)-2-(2-(2,4-dihydroxyphenyl)-acetamido)-3-(1*H*-indol-2-yl)propanamido)heptylamino)-

pentyl)-5-guanidinopentanamide Tetrakis(2,2,2-trifluoroacetate (5h). Yield: 10.8 mg (3.1%). ^{1}H NMR (300 MHz, CD_3OD): δ = 7.63−7.52 (m, 1 H), 7.50 (d, J = 7.9 Hz, 1 H), 7.30 (d, J = 7.9 Hz, 1 H), 7.11−6.93 (m, 3 H), 6.82 (d, J = 8.0 Hz, 1 H), 6.28 (d, J = 2.5 Hz, 1 H), 6.24 (dd, J = 2.5, 8.2 Hz, 1 H), 4.52 (t, J = 6.7 Hz, 1 H), 3.85 (t, J = 6.6 Hz, 1 H), 3.39 (d, J = 3.7 Hz, 2 H), 3.27−3.07 (m, 8 H), 3.02−2.80 (m, 6 H), 1.99−1.81 (m, 2 H), 1.74−1.08 (m, 24 H). ^{13}C NMR (75 MHz, CD_3OD): δ = 175.0, 173.8, 159.0, 157.3, 183.0, 132.7, 128.7, 124.5, 122.5, 119.9, 119.4, 114.1, 112.3, 110.6, 108.1, 103.9, 56.0, 54.3, 41.9, 40.4, 40.3, 38.8, 30.0, 29.9, 29.4, 28.8, 27.2, 27.1, 27.0, 29.6, 25.7, 25.0. HPLC-ELS: 100%. m/z = 708.5 [MH$^+$]. HRMS (EI) exact mass calculated for $C_{32}H_{57}N_9O_5$ [MH$^+$] 708.4561. Found: 708.4545.

(*S*)-*N*^{1}-(4-((8-((*S*)-2-Amino-5-guanidinopentanamido)octyl)-amino)butyl)-2-(2-(2-hydroxyphenyl)acetamido)succinamide Tris(2,2,2-trifluoroacetate (8a). Yield: 66.8 mg (23%). ^{1}H NMR (300 MHz, CD_3OD): δ = 7.04−7.19 (m, 2 H), 6.75−6.88 (m, 2 H), 4.56−4.69 (m, 1 H), 3.86 (t, J = 6.2 Hz, 1 H), 3.61 (d, J = 15.1 Hz, 1 H), 3.53 (d, J = 14.9 Hz, 1 H), 3.22 (t, J = 6.2, 6 H), 2.88 (t, J = 7.4, 4 H), 2.63−2.79 (m, 2 H), 1.78−1.97 (m, 2 H), 1.43−1.78 (m, 10 H), 1.36 (s, 8 H). ^{13}C NMR (75 MHz, CD_3OD): δ = 173.9, 173.6, 172.3, 168.6, 157.6, 155.4, 131.4, 128.7, 122.2, 120.0, 115.3, 53.2, 51.2, 47.9, 47.5, 40.8, 39.8, 38.4, 36.4, 29.3, 29.2, 28.9, 27.0, 26.6, 26.4, 26.3, 24.6, 23.2. HPLC-ELS: 100%. m/z = 620.4 [MH$^+$]. HRMS (EI) exact mass calculated for $C_{30}H_{53}N_9O_5$ [MH$^+$] 620.4248. Found: 620.4256.

(*S*)-*N*^{1}-(4-((8-((*S*)-2-Amino-5-guanidinopentanamido)octyl)-amino)butyl)-2-(2-(4-hydroxyphenyl)acetamido)succinamide Tris(2,2,2-trifluoroacetate (8b). Yield: 38.4 mg (13%). ^{1}H NMR (300 MHz, CD_3OD): δ = 7.09 (d, J = 8.3 Hz, 2 H), 6.72 (d, J = 8.3 Hz, 2 H), 4.60 (t, J = 6.5 Hz, 1 H), 3.85 (t, J = 6.2 Hz, 1 H), 3.47 (s, 2 H), 3.13−3.28 (m, 6 H), 2.92 (t, J = 7.57 Hz, 4 H), 2.59−2.76 (m, 2 H), 1.77−1.98 (m, 2 H), 1.44−1.75 (m, 10 H), 1.37 (s, 8 H). ^{13}C NMR (75 MHz, CD_3OD): δ = 174.7, 174.7, 173.3, 169.7, 158.7, 157.5, 131.3, 127.3, 116.4, 54.2, 52.3, 49.0, 48.5, 42.8, 41.9, 40.8, 39.4, 37.8, 30.4, 30.3, 30.0, 28.1, 27.7, 27.4, 27.4, 25.6, 24.3. HPLC-ELS: 98%. m/z = 620.4 [MH$^+$]. HRMS (EI) exact mass calculated for $C_{30}H_{53}N_9O_5$ [MH$^+$] 620.4248. Found: 620.4234.

(*S*)-*N*^{1}-(4-((8-((*S*)-2-Amino-5-guanidinopentanamido)octyl)-amino)butyl)-2-(2-phenylacetamido)succinamide Tris(2,2,2-htrifluoroacetate (8c). Yield: 41.9 mg (15%). ^{1}H NMR (300 MHz, CD_3OD): δ = 7.10−7.30 (m, 5 H), 4.58 (t, J = 6.5 Hz, 1 H), 3.82 (t, J = 6.3, 1 H), 3.55 (s, 2 H), 3.08−3.24 (m, 6 H), 2.79−2.97 (m, 4 H), 2.55−2.75 (m, 2 H), 1.71−1.94 (m, 2 H), 1.41−1.70 (m, 12 H), 1.32 (s, 10 H). ^{13}C NMR (75 MHz, CD_3OD): δ = 174.6, 174.0, 173.3, 169.7, 136.7, 130.2 (2 C), 129.6 (2 C), 128.0, 54.2, 52.3, 49.0, 48.5, 43.6, 41.8, 40.8, 39.4, 37.9, 37.9, 30.4, 30.3, 29.9, 28.0, 27.7, 27.4, 27.4, 27.4, 25.6, 24.3. HPLC-ELS: 99%. m/z = 604.4 [MH$^+$]. HRMS (EI) exact mass calculated for $C_{30}H_{53}N_9O_4$ [MH$^+$] 604.4299. Found: 604.4290.

2-(2-(1*H*-Indol-3-yl)acetamido)-*N*^{1}-(4-(8-(2-amino-5-guanidinopentanamido)octylamino)butyl)succinamide Tetrakis(2,2,2-trifluoroacetate (8d). Yield: 17.1 mg (5.2%). ^{1}H NMR (300 MHz, CD_3OD): δ = 7.54 (d, J = 7.6 Hz, 1 H), 7.35 (d, J = 8.0 Hz, 1 H), 7.20 (s, 1 H), 7.11 (t, J = 7.6 Hz, 1 H), 7.02 (t, J = 7.3 Hz, 1 H), 4.61 (t, J = 6.5 Hz, 1 H), 3.84 (t, J = 6.7 Hz, 1 H), 3.73 (s, 2 H), 3.28−3.05 (m, 8 H), 2.88 (s, 1 H), 2.85−2.71 (m, 4 H), 2.68 (d, J = 6.4 Hz, 2 H), 1.9 −1.79 (m, 2 H), 1.73−1.29 (m, 22 H), 1.25 (d, J = 6.1 Hz, 2 H). ^{13}C NMR (75 MHz, CD_3OD): δ = 174.9, 174.8, 173.3, 169.6, 138.2, 128.5, 125.2, 122.7, 120.2, 119.4, 112.6, 109.3, 54.2, 52.2, 48.5, 41.9, 40.8, 39.3, 37.5, 34.0, 30.4, 30.3, 30.0, 28.1, 27.7, 27.4, 27.2, 25.7, 24.2, 22.5. HPLC-ELS: 99%. m/z = 643.5 [MH$^+$]. HRMS (EI) exact mass calculated for $C_{32}H_{54}N_{10}O_4$ [MH$^+$] 643.4408. Found: 643.4405.

(*S*)-2-Amino-*N*-(8-((4-((*S*)-2-(2-(2,4-dihydroxyphenyl)-acetamido)propanamido)butyl)amino)octyl)-5-guanidinopentanamide Tris(2,2,2-trifluoroacetate (8e). Yield: 76.4 mg (27%). ^{1}H NMR (300 MHz, CD_3OD): δ = 6.93 (d, J = 8.0 Hz, 1 H), 6.33 (d, J = 1.7 Hz, 1 H), 6.27 (dd, J = 1.7, 7.8 Hz, 1 H), 4.19 (q, J = 7.0 Hz, 1 H), 3.85 (t, J = 6.2 Hz, 1 H), 3.51 (d, J = 14.8 Hz, 1 H), 3.39 (s, 1 H), 3.04−3.29 (m, 6 H), 2.70−2.95 (m, 4 H), 1.75−1.97 (m, 1 H), 1.42−1.75 (m, 10 H), 1.36 (s, 13 H). ^{13}C NMR (75 MHz, CD_3OD): δ = 175.4, 175.3, 169.7, 158.9, 158.7, 157.3, 132.9, 114.5, 107.9, 103.8, 54.2, 51.4, 50.0, 41.8, 40.8, 39.2, 38.5, 30.4, 30.3, 29.9, 28.0, 27.6, 27.4, 27.4, 25.6, 24.3, 17.9. HPLC-ELS: 100%. m/z = 593.4 [MH$^+$]. HRMS (EI) exact mass calculated for $C_{29}H_{52}N_8O_5$ [MH$^+$] 593.4139. Found: 593.4138.

(6*S*,24*S*)-1,6-Diamino-24-(2-(2,4-dihydroxyphenyl)-acetamido)-1-imino-7,23-dioxo-2,8,17,22-tetraazahexacosan-26-oic Acid Tris(2,2,2-trifluoroacetate (8f). Yield: 49.3 mg (17%). ^{1}H NMR (300 MHz, CD_3OD): δ = 6.91 (d, J = 8.2 Hz, 1 H), 6.31 (d, J = 2.5 Hz, 1 H), 6.25 (dd, J = 2.5, 8.1 Hz, 1 H), 4.56 (t, J = 6.2 Hz, 1 H), 3.82 (t, J = 6.5 Hz, 1 H), 3.48 (d, J = 14.9 Hz, 1 H), 3.39 (d, J = 15.1 Hz, 1 H), 3.11−3.26 (m, 6 H), 2.86 (t, J = 7.8 Hz, 4 H), 2.73−2.80 (m, 2 H), 1.74−1.95 (m, 2 H), 1.43−1.72 (m, 10 H), 1.34 (s, 8 H). ^{13}C NMR (75 MHz, CD_3OD): δ = 175.4, 174.1, 173.2, 169.7, 159.0, 157.3, 133.0, 114.3, 108.0, 103.8, 54.2, 51.9, 49.0, 41.8, 40.8, 39.4, 38.8, 36.5, 30.4, 30.3, 30.0, 28.0, 27.7, 27.4, 27.3, 25.6, 24.3. HPLC-ELS: 100%. m/z = 637.4 [MH$^+$]. HRMS (EI) exact mass calculated for $C_{30}H_{52}N_8O_7$ [MH$^+$] 637.4037. Found: 637.4036.

(*S*)-2-Amino-*N*-(8-((4-((*S*)-2-(2-(2,4-dihydroxyphenyl)-acetamido)-3-(1*H*-imidazol-5-yl)propanamido)butyl)amino)-octyl)-5-guanidinopentanamide Tetrakis(2,2,2-trifluoroacetate (8g). Yield: 69.9 mg (21%). ^{1}H NMR (300 MHz, CD_3OD): δ = 8.68 (s, 1 H), 7.12 (s, 1 H), 6.83 (d, J = 8.0 Hz, 1 H), 6.28 (d, J = 2.5 Hz, 1 H), 6.22 (dd, J = 2.5, 8.0 Hz, 1 H), 4.54 (q, J = 5.3 Hz, 1 H), 3.81 (t, J = 6.4 Hz, 1 H), 3.37 (s, 2 H), 3.14−3.25 (m, 6 H), 2.96−3.13 (m, 2 H), 2.88 (t, J = 7.7 Hz, 4 H), 1.75−1.95 (m, 2 H), 1.44−1.69 (m, 10 H), 1.32 (s, 8 H). ^{13}C NMR (75 MHz, CD_3OD): δ = 175.4, 172.2, 169.7, 159.0, 157.2, 134.8, 132.7, 131.2, 118.3, 114.2, 108.0, 103.8, 54.2, 54.1, 49.1, 41.8, 40.8, 39.7, 38.6, 30.4, 30.3, 30.0, 28.1, 27.9, 27.7, 27.4, 27.4, 25.6, 24.5. HPLC-ELS: 99%. m/z = 659.4 [MH$^+$]. HRMS (EI) exact mass calculated for $C_{32}H_{54}N_{10}O_5$ [MH$^+$] 659.4357. Found: 659.4355.

(*S*)-2-Amino-*N*-(8-(4-((*S*)-2-(2-(2,4-dihydroxyphenyl)-acetamido)-3-(1*H*-indol-2-yl)propanamido)butylamino)octyl)-5-guanidinopentanamide Tetrakis(2,2,2-trifluoroacetate (8h). Yield: 29.4 mg (8.4%). ^{1}H NMR (300 MHz, CD_3OD): δ = 7.49 (d, J = 7.96 Hz, 1 H), 7.30 (d, J = 8.3 Hz, 1 H), 7.06 (t, J = 7.3, 1 H), 7.01−6.91 (m, 2 H), 6.82 (d, J = 8.3 Hz, 1 H), 6.28 (d, J = 2.4 Hz, 1 H), 6.24 (dd, J = 2.5, 8.03 Hz, 1 H), 4.45 (t, J = 6.7 Hz, 1 H), 3.83 (t, J = 6.6 Hz, 1 H), 3.39 (s, 2 H), 3.28−3.09 (m, 8 H), 3.08−2.94 (m, 1 H), 2.92−2.71 (m, 4 H), 1.96−1.74 (m, 2 H), 1.72−1.29 (m, 20 H). ^{13}C NMR (75 MHz, CD_3OD): δ = 172.6, 171.6, 167.0, 156.4, 154.6, 135.4, 130.1, 126.0, 122.0, 119.9, 117.2, 116.7, 111.5, 109.7, 107.9, 105.4, 101.2, 53.7, 51.6, 39.2, 38.2, 36.7, 36.0, 27.8, 27.7, 27.3, 26.0, 25.4, 25.1, 24.8, 24.6, 23.0, 21.6. HPLC-ELS: 100%. m/z = 708.5 [MH$^+$]. HRMS (EI) exact mass calculated for $C_{32}H_{57}N_9O_5$ [MH$^+$] 708.4561. Found: 708.4559.

Electrophysiology. In Vitro cRNA Transcription. The cDNA encoding rat GluA1$_i$ or GluN1/2A subunits were inserted into the vectors pGEM-HE or pCIneo, respectively, for preparation of high-expression cRNA transcripts. Plasmids were grown in Top10 *E. coli* bacteria (Invitrogen, Carlsbad, CA) and isolated by using column purification (Qiagen, La Jolla, CA). The cRNA was synthesized from the above cDNAs by in vitro transcription using the mMESSAGE mMACHINE T7 mRNA-capping kit (Ambion, Austin, TX) according to the protocol supplied by the manufacturer.

Oocyte Electrophysiology. Mature female *Xenopus laevis* (Nasco, Modesto, CA) were anesthetized using 0.1% ethyl 3-aminobenzoate, and their ovaries were surgically removed. The ovarian tissue was dissected and treated with collagenase in Ca^{2+}-free Barth's medium (2 mg/mL) for 1−2 h at room temperature. On the second day, oocytes were injected with 25 nL of cRNA (1 ng/nL for GluA1$_i$ or 0.05 ng/nL for GluN1/2A) and incubated at 17 °C in Barth's medium (in mM: 88 NaCl, 1 KCl, 0.33 $Ca(NO_3)_2$, 0.41 $CaC1_2$, 0.82 $MgSO_4$, 2.4 $NaHCO_3$, 10 HEPES; pH 7.4) with gentamicin (0.10 mg/mL). Oocytes were used for recordings after 3−6 days postinjection and were voltage-clamped with the use of a two-electrode voltage clamp (Dagan Corporation, Minneapolis, MN) with both microelectrodes filled with 3 M KCl. Recordings were made while the oocytes were continuously superfused with frog Ringer's solution (in mM: 115 NaCl, 2 KCl, 1.8

$BaC1_2$, 5 HEPES; pH 7.6). The test compounds were dissolved in frog Ringer's solution and added by bath application. Recordings were made at room temperature at holding potentials in the range from −80 to −40 mV. Antagonist concentration−response curves were constructed by measuring the maximal current induced by the saturating concentration of agonist (300 μM glutamate for $GluA1_i$; 100 μM glutamate and 100 μM glycine for GluN1/N2A) and then applying increasing concentrations of antagonist in the presence of the appropriate agonist. Data from individual oocytes were fitted to the equation $I = I_{min} + [(I_{max} - I_{min})/(1 + ([antagonist]/IC_{50})^{n_H})]$, where I is the agonist-evoked current at a given antagonist concentration, I_{max} is the agonist-evoked current in the absence of antagonist, I_{min} is the agonist-evoked current in the presence of the highest antagonist concentration, [antagonist] is the concentration of antagonist, and n_H is the Hill slope. The IC_{50} (concentration of antagonist producing 50% of I_{max}) values were determined by an iterative least-squares fitting routine. Concentration−response curves were determined in triplicate for three to eight individual oocytes.

■ ASSOCIATED CONTENT

Ⓢ Supporting Information

Tables S1, S2, S3, and S4 listing IC_{50} values. This material is available free of charge via the Internet at http://pubs.acs.org.

■ AUTHOR INFORMATION

Corresponding Author

*Phone: +45 3533 6114. E-mail: kristian.stromgaard@sund.ku.dk.

Present Address

‡Department of Medicinal Chemistry, Boehringer Ingelheim RCV GmbH & Co. KG, A-1121 Vienna, Austria.

Author Contributions

†These authors contributed equally to this work.

Notes

The authors declare no competing financial interest.

■ ACKNOWLEDGMENTS

We are grateful for support from Alfred Benzon Foundation (S.L.), GluTarget (M.H.P.), and the Lundbeck Foundation (K.S.).

■ ABBREVIATIONS USED

ADDP, 1,1-(azodicarbonyl)dipiperidine; AMPA, α-amino-3-hydroxy-5-methyl-4-isoxazolepropionic acid; ArgTX, argiotoxin; DBU, 1,8-diazabicyclo[5.4.0]undec-7-ene; DIPEA, diisopropylethylamine; HATU, 2-(1*H*-7-azabenzotriazol-1-yl)-1,1,3,3-tetramethyluronium hexafluorophosphate; iGlu, ionotropic glutamate; NMDA, *N*-methyl-D-aspartate; Ns, 2-nitrobenzenesulfonamide; Pbf, pentamethyl-2,3-dihydrobenzofuran-5-sulfonyl; TBAF, tetra-*n*-butylammonium fluoride; Teoc, 2-(trimethylsilyl)ethyloxycarbonyl; TEVC, two-electrode voltage clamp

■ REFERENCES

(1) Traynelis, S. F.; Wollmuth, L. P.; Mcbain, C. J.; Menniti, F. S.; Vance, K. M.; Ogden, K. K.; Hansen, K. B.; Yuan, H.; Myers, S. J.; Dingledine, R.; Sibley, D. Glutamate receptor ion channels: structure, regulation, and function. *Pharmacol. Rev.* **2010**, *62*, 405−496.

(2) Mayer, M. L. Emerging models of glutamate receptor ion channel structure and function. *Structure* **2011**, *19*, 1370−1380.

(3) Mayer, M. Glutamate receptors at atomic resolution. *Nature* **2006**, *440*, 456−462.

(4) Lipton, S. A. Paradigm shift in neuroprotection by NMDA receptor blockade: memantine and beyond. *Nat. Rev. Drug Discovery* **2006**, *6*, 160−170.

(5) Parsons, C. G.; Stoffler, A.; Danysz, W. Memantine: a NMDA receptor antagonist that improves memory by restoration of homeostasis in the glutamatergic system—too little activation is bad, too much is even worse. *Neuropharmacology* **2007**, *53*, 699−723.

(6) McKeage, K. Memantine, a review of its use in moderate to severe Alzheimer's disease. *CNS Drugs* **2009**, *23*, 881−897.

(7) Van Marum, R. J. Update on the use of memantine in Alzheimer's disease. *Neuropsychiatr., Dis. Treat.* **2009**, *5*, 237−247.

(8) Strømgaard, K.; Mellor, I. R. AMPA receptor ligands: synthetic and pharmacological studies of polyamines and polyamine toxins. *Med. Res. Rev.* **2004**, *24*, 589−620.

(9) Strømgaard, K.; Jensen, L. S.; Vogensen, S. B. Polyamine toxins: development of selective ligands for ionotropic receptors. *Toxicon* **2005**, *45*, 249−254.

(10) Herlitze, S.; Raditsch, M.; Ruppersberg, J. P.; Jahn, W.; Monyer, H.; Schoepfer, R.; Witzemann, V. Argiotoxin detects molecular differences in AMPA receptor channels. *Neuron* **1993**, *10*, 1131−1140.

(11) Blaschke, M.; Keller, B. U.; Rivosecchi, R.; Hollmann, M.; Heinemann, S.; Konnerth, A. A single amino acid determines the subunit-specific spider toxin block of α-amino-3-hydroxy-5-methyl-isoxazole-4-propionate/kainate receptor channels. *Proc. Natl. Acad. Sci. U.S.A.* **1993**, *90*, 6528−6532.

(12) Pellegrini-Giampietro, D. E.; Gorter, J. A.; Bennett, M. V.; Zukin, R. S. The GluR2 (GluR-B) hypothesis: Ca^{2+}-permeable AMPA receptors in neurological disorders. *Trends Neurosci.* **1997**, *20*, 464−470.

(13) Liu, S. J.; Savtchouk, I. Ca^{2+} permeable AMPA receptors switch allegiances: mechanisms and consequences. *J. Physiol.* **2012**, *590*, 13−20.

(14) Beattie, M. S.; Ferguson, A. R.; Bresnahan, J. C. AMPA-receptor trafficking and injury-induced cell death. *Eur. J. Neurosci.* **2010**, *32*, 290−297.

(15) Eldefrawi, A. T.; Eldefrawi, M. E.; Konno, K.; Mansour, N. A.; Nakanishi, K.; Oltz, E.; Usherwood, P. N. Structure and synthesis of a potent glutamate receptor antagonist in wasp venom. *Proc. Natl. Acad. Sci. U.S.A.* **1988**, *85*, 4910−4913.

(16) Strømgaard, K.; Brierley, M. J.; Andersen, K.; Sløk, F. A; Mellor, I. R.; Usherwood, P. N. R.; Krogsgaard-Larsen, P.; Jaroszewski, J. W. Analogues of neuroactive polyamine wasp toxins that lack inner basic sites exhibit enhanced antagonism toward a muscle-type mammalian nicotinic acetylcholine receptor. *J. Med. Chem.* **1999**, *42*, 5224−5234.

(17) Strømgaard, K.; Brier, T. J.; Andersen, K.; Mellor, I. R.; Saghyan, A.; Tikhonov, D.; Usherwood, P. N. R.; Krogsgaard-Larsen, P.; Jaroszewski, J. W. Solid-phase synthesis and biological evaluation of a combinatorial library of philanthotoxin analogues. *J. Med. Chem.* **2000**, *43*, 4526−4533.

(18) Kromann, H.; Krikstolaityte, S.; Andersen, A. J.; Andersen, K.; Krogsgaard-Larsen, P.; Jaroszewski, J. W.; Egebjerg, J.; Strømgaard, K. Solid-phase synthesis of polyamine toxin analogues: potent and selective antagonists of Ca^{2+}-permeable AMPA receptors. *J. Med. Chem.* **2002**, *45*, 5745−5754.

(19) Jørgensen, M. R.; Olsen, C. A.; Mellor, I. R.; Usherwood, P. N. R.; Witt, M.; Jaroszewski, J. W.; Franzyk, H. The effects of conformational constraints and steric bulk in the amino acid moiety of philanthotoxins on AMPAR antagonism. *J. Med. Chem.* **2005**, *48*, 56−70.

(20) Jensen, L. S.; Bølcho, U.; Egebjerg, J.; Strømgaard, K. Design, synthesis and pharmacological characterization of polyamine toxin derivatives: novel, potent ligands for the pore-forming region of AMPA receptors. *ChemMedChem* **2006**, *1*, 419−428.

(21) Olsen, C. A.; Mellor, I. R.; Wellendorph, P.; Usherwood, P. N. R.; Witt, M.; Franzyk, H.; Jaroszewski, J. W. Tuning wasp toxin structure for nicotinic receptor antagonism: Cyclohexylalanine-containing analogues as potent and voltage-dependent blockers. *ChemMedChem* **2006**, *1*, 303−305.

(22) Andersen, T. F.; Tikhonov, D. B.; Bølcho, U.; Bolshakov, K.; Nelson, J. K.; Pluteanu, F.; Mellor, I. R.; Egebjerg, J.; Strømgaard, K. Uncompetitive antagonism of AMPA receptors: mechanistic insights from studies of polyamine toxin derivatives. *J. Med. Chem.* **2006**, *49*, 5414−5423.
(23) Frølund, S.; Bella, A.; Kristensen, A. S.; Ziegler, H. L; Witt, M.; Olsen, C. A.; Strømgaard, K.; Franzyk, H.; Jaroszewski, J. W. Assessment of structurally diverse philanthotoxin analogues for inhibitory activity on ionotropic glutamate receptor subtypes: discovery of nanomolar, non-selective, and use-dependent antagonists. *J. Med. Chem.* **2010**, *53*, 7741−7451.
(24) Olsen, C. A.; Kristensen, A. S.; Strømgaard, K. Small molecules from spiders as chemical probes. *Angew. Chem., Int. Ed.* **2011**, *50*, 11296−11311.
(25) Grishin, E. V.; Volkova, T. M.; Arseniev, A. S.; Reshetova, O. S.; Onoprienko, V. V.; Magazanik, L. G.; Antonov, S. M.; Fedorova, I. M. Structural−functional characteristics of argiopine—the ion channel blockers from the spider *Argiope lobata* venom. *Bioorg. Khim.* **1986**, *12*, 1121−1124.
(26) Lucas, S.; Poulsen, M. H.; Nørager, N. G.; Barslund, A. F.; Bach, T. B.; Kristensen, A. S.; Strømgaard, K. General synthesis of *β*-alanine-containing spider polyamine toxins and discovery of *Nephila* polyamine toxins 1 and 8 as highly potent inhibitors of ionotropic glutamate receptors. *J. Med. Chem.* **2012**, *55*, 10297−10301.
(27) Green, A.; Nakanishi, K.; Usherwood, P. N. Polyamine amides are neuroprotective in cerebellar granule cell cultures challenged with excitatory amino acids. *Brain Res.* **1996**, *717*, 135−146.
(28) Albensi, B. C.; Alasti, N.; Mueller, A. L. Long-term potentiation in the presence of NMDA receptor antagonist arylalkylamine spider toxins. *J. Neurosci. Res.* **2000**, *62*, 177−185.
(29) Nelson, J. K.; Frølund, S. U.; Tikhonov, D. B.; Kristensen, A. S.; Strømgaard, K. Synthesis and biology of argiotoxin-636 and analogues: selective antagonists for ionotropic glutamate receptors. *Angew. Chem., Int. Ed.* **2009**, *49*, 3087−3091.